Experimental and numerical analysis of flow through catalytic converters for original part and WALKER's replacement using reverse engineering and CFD

D Kurzydym[1,2] **A Klimanek**[1] **and Z Żmudka**[1]

[1] Silesian University of Technology, Institute of Thermal Technology, Gliwice, Poland
[2] Tenneco Automotive Polska Sp. z o.o., Aftermarket Engineering, Rybnik, Poland

E-mail: dkurzydym@tenneco.com

Abstract. The paper describes results of experiments and CFD simulation for an original catalytic converter part and WALKER's replacement. Pressure drop was measured for catalysts, which influences on exhaust backpressure, an important parameter affecting the engine power, fuel consumption, emission of harmful gases and wear components. First the pressure drops was examined in the original catalyst and in prototypes of WALKER's. The prototypes differed in that their monoliths had different lengths, density of channels and contents of precious metals (PGM). In the next stage reverse engineering was applied, which included laser scanning of parts and then processing the point clouds in Leios2 program. Recreated 3D geometry of catalysts in Catia v5 program was prepared for computational fluid dynamics. For all studied cases the measured data were used to calculate coefficients of porous media model i.e. viscous and inertial resistances, which were used in the Ansys Fluent program. Static pressure drops on the monoliths were then predicted by the CFD model for different gas mass flow rates through the catalysts. Exhaust velocities and flow uniformity were also analysed. Comparison of the results for all parts allowed for stating, which prototype is better and which has operating parameters comparable to the original part.

1. Introduction

Reducing the emission of toxic substances is an important problem of modern automotive industry due to the significant share of transport in environmental pollution and human health. Progressive process of tightening emission standards forces car manufacturers to develop exhaust aftertreatment systems, that enable to meet future standards. In order to reduce emissions and fulfillment of standards, catalytic converters are commonly used in cars thereby continuously improved and used in various combinations, which is confirmed by numerous scientific studies [1, 2, 3].

A catalytic converter contains a honeycomb monolith with a network structure of parallel channels through which gases flow. The substrate has coating of washcoat (γ–Al_2O_3) which increases porosity of channel walls and at the same time it plays a role of the carrier for active catalysts layer i.e. PGM – platinum group metal (e.g. Pt, Pd, Rh) [1, 2, 3].

Catalysts must meet a number of requirements: having a small thermal capacity, high mechanical and chemical resistance, resistance to thermal shocks and vibrations as well as constant activity during changes in the composition of gases treatment. They should also have good thermal conductivity in order to allow the catalyst rapidly warm up to working temperature ("light-off") which ensures adequate catalytic activity [4].

Currently the most known is a three-way catalytic converter (figure 1) in which reduction and oxidation of harmful flue gas components into non-toxic gases are performed by the following chemical reactions simultaneously at stoichiometric conditions [1, 2]:

- major oxidation reactions of incomplete combustion products i.e. carbon monoxide and unburned hydrocarbons:

$$2CO + O_2 \Rightarrow 2CO_2 \tag{1}$$

$$C_mH_n + \left(m + \frac{n}{4}\right)O_2 \Rightarrow mCO_2 + \frac{n}{2}H_2O \tag{2}$$

- major reduction reactions of nitrogen oxides:

$$2NO + 2CO \Rightarrow N_2 + 2CO_2 \tag{3}$$

$$2NO_2 + 2CO \Rightarrow N_2 + 2CO_2 + O_2 \tag{4}$$

The physical and chemical phenomena (multi-physics and multi-scale) take place inside the monolith substrate channels involving energy, mass and momentum transfer as well as heterogeneous kinetics of the reactions. The efficiency of the monolith converter depends on these phenomena. Two approaches can be considered i.e. macroscopic scales (substrate and channels) and molecular scales (washcoat and catalytically activity surface). In the gas phase (figure 1) convective and diffusive transport of mass, momentum and energy appear in axial and radial directions. The energy balance of the solid is affected by diffusive transport (conduction) as well as radiation and chemical reactions in gas phase and within the catalytic porous surface (adsorption - surface reactions - desorption) called exothermic reactions. Heat transfer mechanisms consist of heat conduction along the monolith, heat from reactions, convection of chemical compounds in the gas phase and thermal radiation [5, 6].

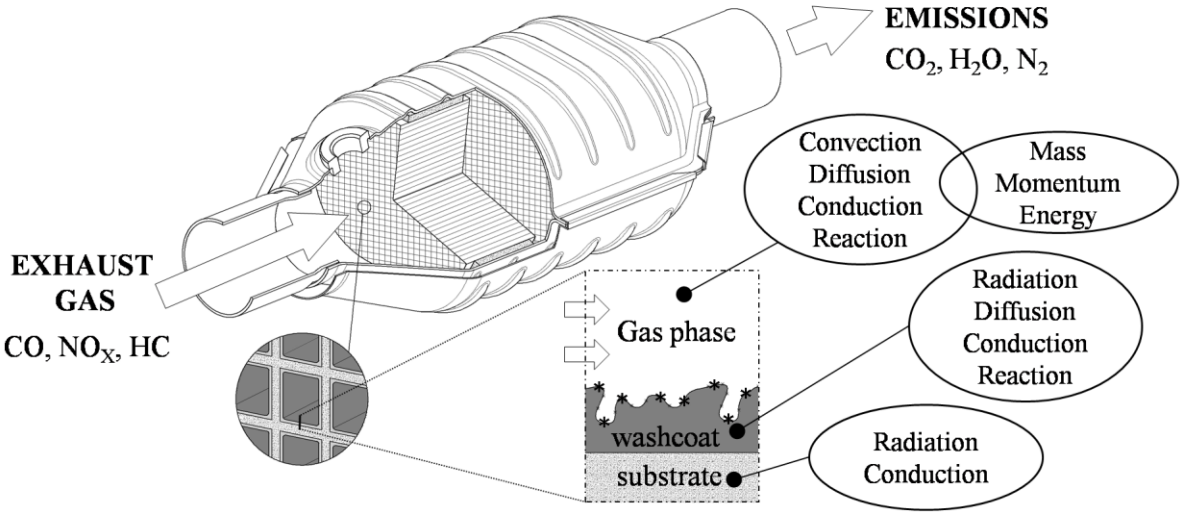

Figure 1. Schematic of catalytic converter with physical and chemical phenomena.

With reference to engine's charge exchange work, there are two important aspects of the catalytic converter operation. The first of them – ecological aspect (favorable), refers to reduction of harmful emissions what was mentioned. The second one is the energy aspect (negative) consisting in the increase of the flow resistance in the exhaust system. Rise both the flow resistance of fresh charge as well as exhaust gases, increases charge exchange work while contributing to reduction of internal and effective work of the engine. This situation also leads to lower effective efficiency of the engine, especially in the field of partial loads. In the model approach, the catalytic converter can be treated as an element of local (detailed constructional data of converter are unknown) and linear (linear resistance with energy dissipation along the exhaust flow) resistance of exhaust system [7].

2. Experiments

The objective of the research was to determine the pressure drop in catalysts, which refers to the static pressure drop of gases moving through obstructions (monolith). The pressure drop was measured against the direction of flow. The average pressure in the exhaust pipe during the exhaust stroke is meant as the exhaust pressure and the atmospheric pressure is the ambient pressure. The difference between these two pressures is commonly defined as exhaust backpressure [8]. In other words, the exhaust backpressure can be defined as the resistance pressure imposed on the engine due to the resistance of the exhaust system in facilitating the flow from engine to the outside ambient [9]. Flow resistance generated by a converter can be considered as a local resistance (Darcy model) [10]:

$$\Delta p = \xi \frac{w_{0,ex}^2}{2v_{ex}} \tag{5}$$

where:

Δp, *Pa*– pressure drop; ξ – resistance factor of the catalyst; $w_{0,ex}$, m/s – average velocity of exhaust gas in the catalyst; v_{ex}, m^3/kg – average specific volume of exhaust gas within the catalyst.

Relationship of the resistance factor and Reynolds number $\xi = f(\mathrm{Re})$ can be determined because the resistance factor decreases as inflow Reynolds number of exhaust gases increases [10].

Backpressure is a scalar quantity, not a vector quantity, and has no direction. The gas flows in one direction only, and the flow is driven by pressure gradient with the only possible direction of flow being that from a higher to a lower pressure [11]. Backpressure should be used to denote exhaust pressure at the exhaust manifold, which is equal to the exhaust gas pressure drop over the whole exhaust system. In accordance with the terminology used in fluid dynamics, the use of the term as in experimental practice "catalytic converter backpressure" in favour of "catalytic converter pressure drop or loss" should be avoided.

An increase in exhaust backpressure decreases NO_X, due to the increased exhaust gas remaining in the cylinder. Excessive backpressure in the exhaust system creates overmuch heat (e.g. exhaust valves and turbine), lowers engine power output (0,3 kW of power per 10 mbar of pressure loss) and fuel consumption in the engine cylinder, that may cause poor performance (e.g. reduced intake manifold boost pressure, cylinder scavenging and combustion effect) and damage of the engine parts (e.g. turbocharger problems – seals, increased pumping work etc.). Therefore backpressure in a certain level (specified by the engine manufacturer) contributes to improvement of the engine performance and reduces emissions [8, 11, 12, 13].

Experimental measurements were made in a laboratory test facility. The test stand, presented in figure 2, consisted of feed tube with mass flowmeter of air inflow (in 8 growing values) and micro manometer (for static pressure – pressure loss) installed on the inlet side. In addition, the stand allows also for measuring the temperature of air at the inlet of feed tube and ambient temperature and pressure. The results were collected on a computer in Excel files through the LabVIEW software.

The object of the study was OEM (Original Equipment Manufacturer) catalytic converter for Ford Focus 1.6 EcoBoost 110 kW and its spare part for Aftermarket from WALKER brand - six prototypes with different properties of monoliths (table 1). For each part, the experimental results were collected for further analysis i.e. for calculation of coefficients for CFD simulations.

Figure 2. Measurements in a laboratory test facility: original part (left), prototype A (right).

Table 1. Properties of the monoliths used.

Part	Diameter × Length (inch)	Cell density (cell/inch^2)	PGM loading (g/ft^3)	Weight ratio (Pt:Pd:Rh)	Wall thickness (mm)
OE part	4.66 × 4	400	N/A	N/A	N/A
Prototype A	4.66 × 3	400	40	0:3:1	0.18
Prototype B	4.66 × 3	400	40	0:2:1	0.18
Prototype C	4.66 × 4	400	40	0:3:1	0.18
Prototype D	4.66 × 4	400	50	0:3:1	0.18
Prototype E	4.66 × 4	400	60	0:3:1	0.18
Prototype F	4.66 × 4	600	30	0:3:1	0.11

3. Reverse engineering

The process of duplicating an existing part without drawings, documentation or a computer model is known as reverse engineering (RE). In other words, RE is also defined as the process of obtaining a geometric CAD model from 3D points from scanning or digitizing existing part. The generic process of RE is composed of three-phases: scanning, point processing and 3D model development [14].

At the beginning part geometries (OE and AM) have been scanned (figure 3) by noncontact scanning technology in order to obtain cloud of points from parts, which define the surface geometry. A laser scanner (ROMER Absolute Arm RA-7530) was used which has a measuring range of 3 m and point repeatability 0.03 mm. The output of the scanning were points clouds data from the Metrolog X4 software as raw data of points (X, Y, Z) in TXT format file.

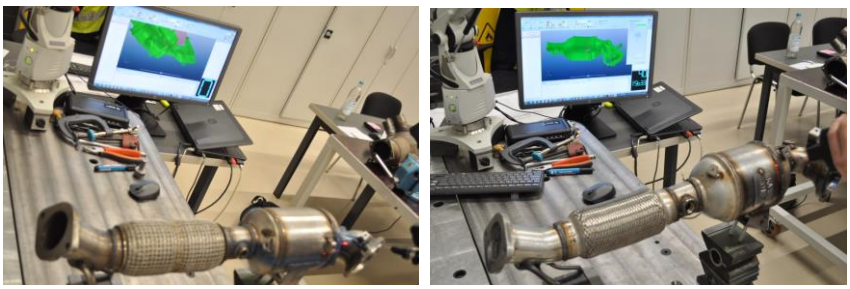

Figure 3. Parts scanning in the 3D laboratory: original part (left), prototype A (right).

The next step was importing the point cloud data to the Leios 2 software as presented in figure 4, where cleaning of noise in the collected data and reduction of the number of points were applied. Triangle meshes were made using built-in tools and cross-sections as NURBS (Non-uniform rational B-spline) were generated, which were the basis for the next stage of model reconstruction.

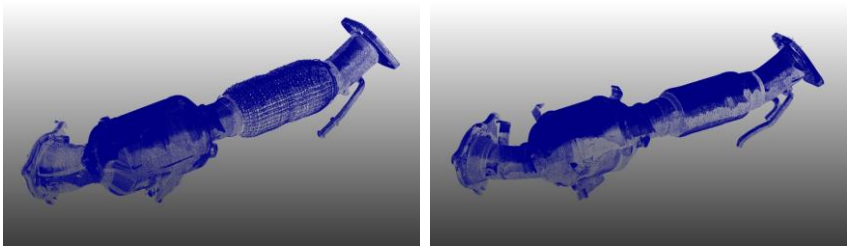

Figure 4. Points cloud in the Leios 2 program: original part (left), prototype A (right).

The last stage of the RE process was generation of 3D models in Catia v5 based on prepared base geometry from Leios 2 (cross-sections splines, points and planes). The 3D models ware made in the Generative Shape Design module and then Part Design module. The generated 3D models are presented in figure 5.

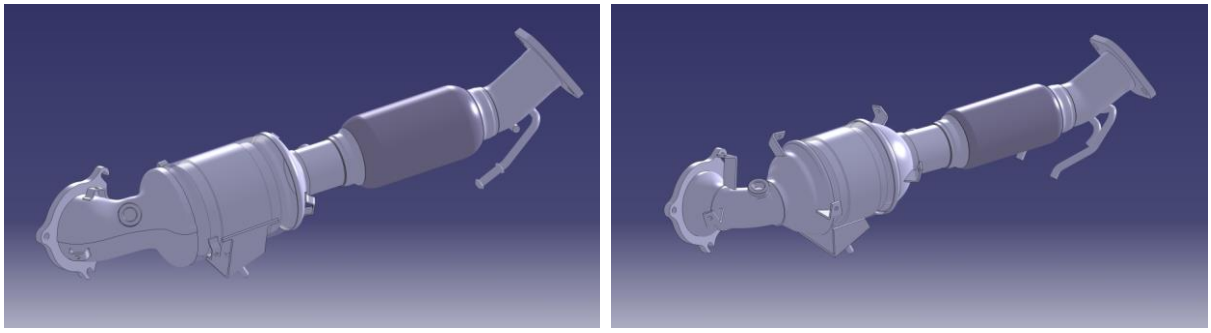

Figure 5. 3D models in Catia v5: original part (left), prototype A (right).

In addition, thanks to the capabilities of the Leios 2 software, inspections of the models have been carried out i.e. the point cloud with the finished reconstructed 3D model have been compared. The results of the comparison are presented in figure 6, where the point clouds are shown against the 3D models. The most important geometrical features have been reproduced in tolerance ±0.5mm which is enough for CFD simulations.

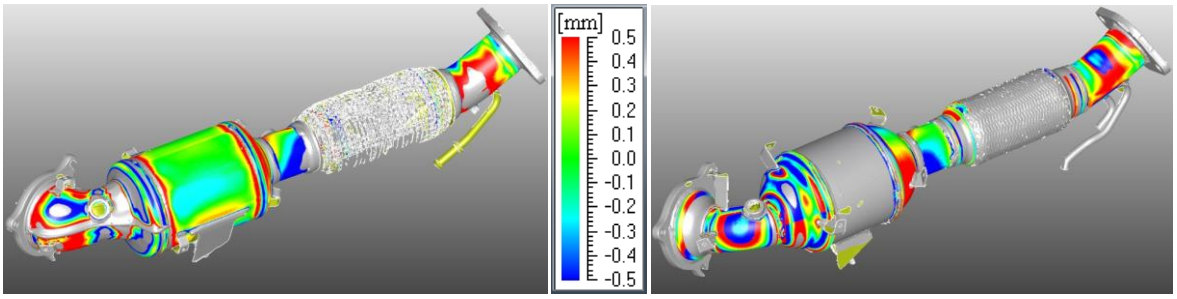

Figure 6. Deviations of point clouds vs. 3D models: original part (left), prototype A (right).

4. CFD modeling

In order to prepare computational fluid dynamics (CFD) simulations first, internal geometries of catalysts were created from 3D models. All the insignificant details in the geometry models have been simplified e.g. edges, fillets, grooves, etc. This allowed for a better mesh adjustment, and generation of tetrahedral mesh for inlet and outlet side, while hexahedral mesh was used for the monolith. The size of the elements was 4E-03 m, what gave the total number of 460 thousand mesh elements in the whole 3D model (figure 7).

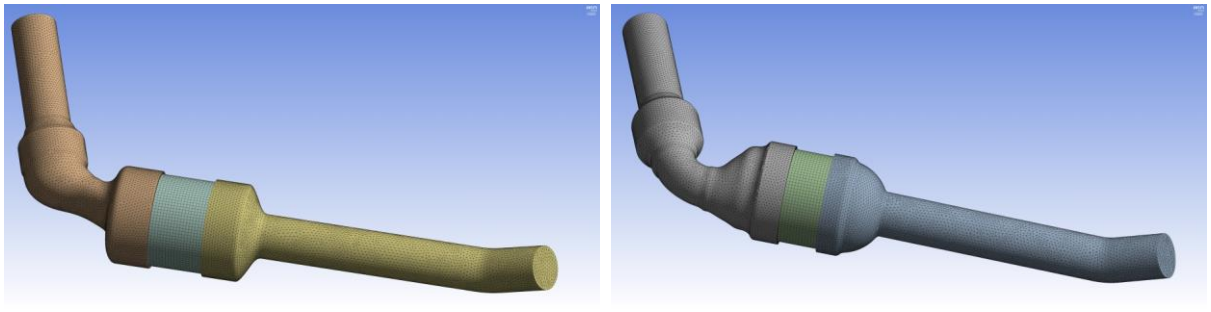

Figure 7. Simplified 3D models with mesh: original part (left), prototype A (right).

Modeling of flow through the catalytic converter was carried out using the Ansys Fluent CFD package. CFD simulations offer an opportunity to minimize cost and time consumption due to avoidance experimental tests. Ansys Fluent was used to provide detailed information on the flow field as function of various design and operating parameters [15, 16].

Steady state flow simulations through the catalytic converter were performed. The flow inside the anisotropic porous medium (monolith) was treated as laminar due to very small hydraulic diameter of the flow channels, whereas in the remaining volume of flow domain the turbulence was modelled by means of the realizable $k-\varepsilon$ model with standard wall functions approach for near-wall treatment. The k-epsilon turbulence model is based on model of transport equations for the turbulent kinetic energy k and its dissipation rate ε [15, 16].

The governing equations for the flow within the domain are the Reynolds Averaged Navier-Stokes (RANS) equations. The total mass conservation equation (continuity equation), is [15, 16]:

$$\frac{\partial \rho}{\partial t} + \nabla \cdot \left(\rho \vec{v} \right) = 0 \tag{6}$$

where:

$\rho,\ kg/m^3$ - density; $t,\ s$ - time; $\vec{v},\ m/s$ - fluid velocity vector.

The momentum conservation equation called volume average Navier-Stokes (VANS), is [15,16]:

$$\frac{\partial}{\partial t}\left(\rho \vec{v} \right) + \nabla \cdot \left(\rho \vec{v}\vec{v} \right) = -\nabla p + \nabla \cdot \left(\bar{\bar{\tau}} \right) + \rho \vec{g} + S_i \tag{7}$$

where:

$p,\ Pa$ - pressure; $\tau,\ Pa$ - stress tensor; $\vec{g},\ m/s^2$ - gravitational acceleration; S_i - body force (source term).

As mentioned above the equations were solved in steady state, thus the first terms in equation (6) and (7) were omitted. The gravitational acceleration appearing in equation (7) was also neglected. For the porous zone, the velocity is replaced with the superficial velocity, which is equal to the fluid physical velocity inside the porous zone multiplied by the medium porosity. The source term S_i of the external body force was non-zero in the porous media zone only and was modelled using the Darcy-Forcheimer for simple homogenous porous medium [16, 17]:

$$S_i = \frac{\Delta p}{\Delta L_i} = -\left(\frac{\mu}{\alpha} v_i + C_2 \frac{1}{2} \rho v_i^2 \right) \tag{8}$$

where:

$\Delta p,\ Pa$ - pressure drop; $\mu,\ Pa \cdot s$ - laminar fluid viscosity; $\alpha,\ m^2$ - permeability of the medium; $C_2,\ 1/m$ - inertial resistance; $v_i,\ m/s$ - velocity normal to the porous face in one specific direction; $\rho,\ kg/m^3$ - density; $\Delta L_i,\ m$ - thickness of the medium in one specific direction.

As seen in equation (8), the first part accounts for viscous resistance (viscous loss), with a proportionality coefficient $1/\alpha$ and the second term accounts for inertial resistance (inertial loss) with inertial resistance coefficient C_2. To find the viscous and inertial resistance coefficients for a porous material, a pressure drop correlation $\Delta p = f(v)$ modelled with a quadratic polynomial function was determined from the experiments. From equation (8), it may be noticed that a source term will also take the form of parabolic function, which in general can be written in the form [17, 18]:

$$\Delta p = a v_i^2 + b v_i \tag{9}$$

Comparing equations (8) with (9), the viscous and inertial resistance coefficients can be calculated from the following relations [17]:

$$\frac{1}{\alpha} = \frac{b}{\mu \Delta L_i} \tag{10}$$

$$C_2 = \frac{2a}{\rho \Delta L_i} \tag{11}$$

The experimentally determined pressure drops were used to calculate the coefficients $1/\alpha$ and C_2. These in turn were used in the CFD simulation which allowed for predicting the flow in the model.

5. Results

After the CFD simulations for original part and six prototypes, experimental and numerical results were compared as presented in figure 8. The presented polynomials from experimental results on the plot were used to calculate the viscous and inertial resistance according to equation (10) and (11). Percentage relative error (PRE) in figure 8 was defined as:

$$PRE = \frac{\Delta p_{\text{exp}} - \Delta p_{\text{mod}}}{\Delta p_{\text{exp}}} \times 100\% \tag{12}$$

where:

Δp_{exp}, Pa - measured pressure drop; Δp_{mod}, Pa - pressure drop predicted by the CFD model.

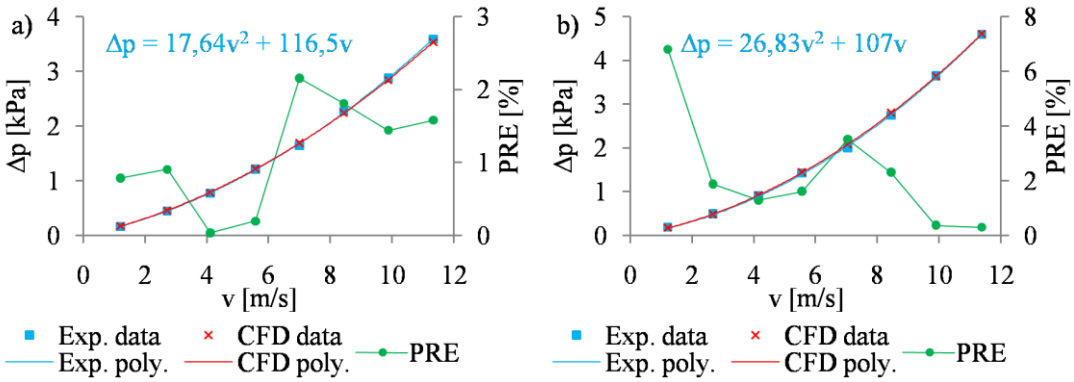

Figure 8. Pressure drop vs. velocity (experimental vs. CFD data): a) original part, b) prototype A.

The average of PRE is the percentage mean relative error (PMRE), which for all the analyzed cases did not exceed 3 %. The experimental results for tested parts are summarized in figure 9.

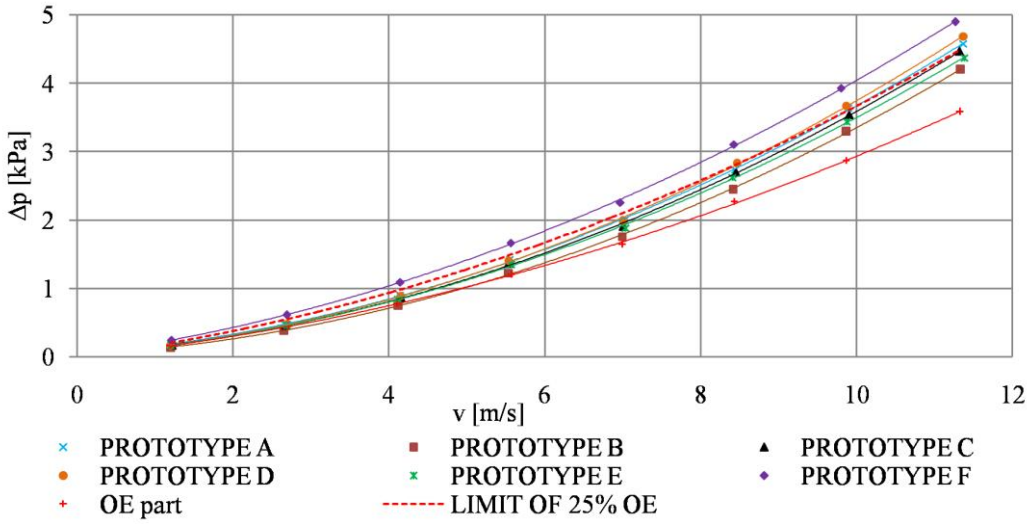

Figure 9. Experimental data of pressure drop vs. velocity for original part and prototypes.

The red line in the figure 9 means that the value of backpressure from aftermarket part shall not exceed the value of original part by more than 25 % according directive 70/157/EEC.

For initial values of mass flow rate (e.g. 0.016 kg/s), CFD model became convergent (with small residuals) and stable (on the outlet side) after about 600 iterations. However, for large mass flow rate (e.g. 0.15 kg/s), CFD model was stable after about 200 iterations. Figure 10 shows a comparison of parts with the pressure drop fields for the initial mass flow rate 0.016 kg/s.

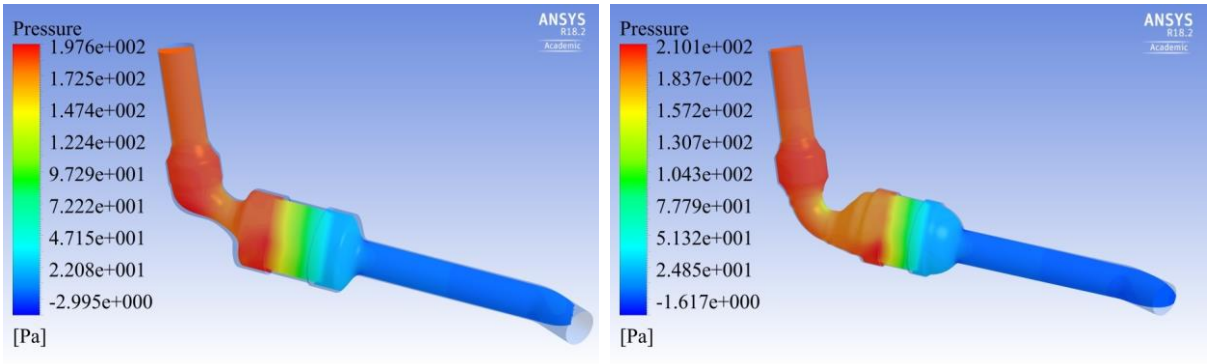

Figure 10. CFD results of pressure drop: original part (left), prototype A (right).

Subsequently, figure 11 shows a comparison of velocity streamlines. It is possible to notice, where in the geometry the greatest velocities and the fluid recirculation before entering to the monolith are.

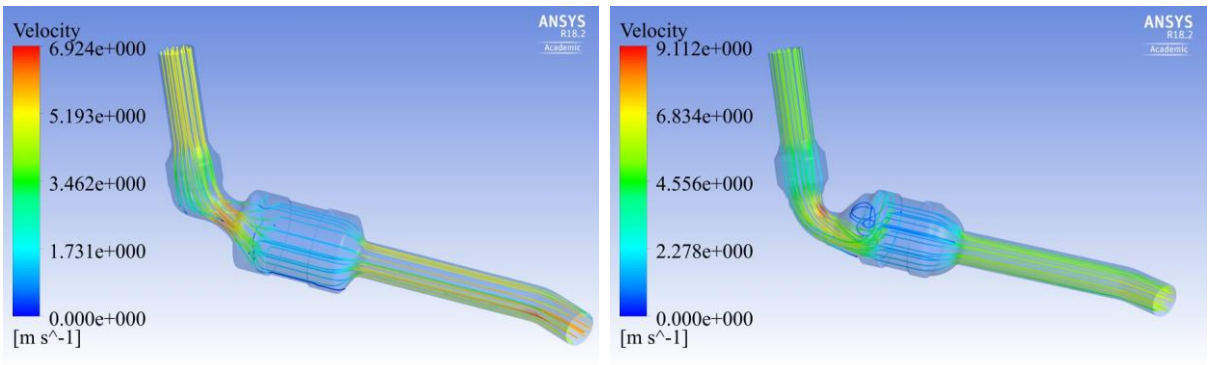

Figure 11. CFD results of velocity: original part (left), prototype A (right).

The flow distribution, through the monolith affects the conversion efficiency, catalyst utilization and faster "light-off" during the cold start period. Therefore, design goals include a minimum pressure drop with an ideal flow uniformity index of 1. Figure 12 presents flow velocity variations across the inlet face of the monolith, where for original part uniformity index was 0.89 and for aftermarket 0.88.

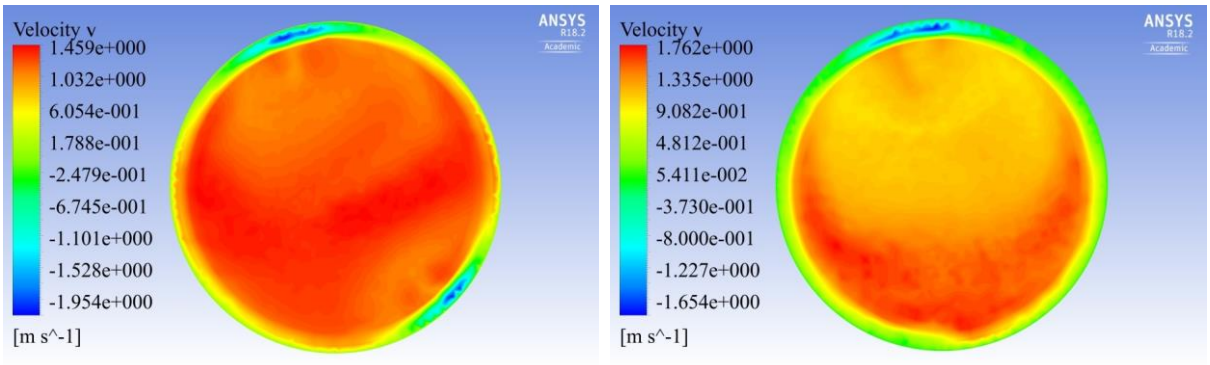

Figure 12. CFD results of velocity - front wall of monolith: original part (left), prototype A (right).

In figure 13 the velocity across the porous substrate and also pressure drop are presented. The pressure changes rapidly, where the fluid velocity changes as it passes through the monolith. The pressure drop can be high, due to the inertial and viscous resistance of the porous media.

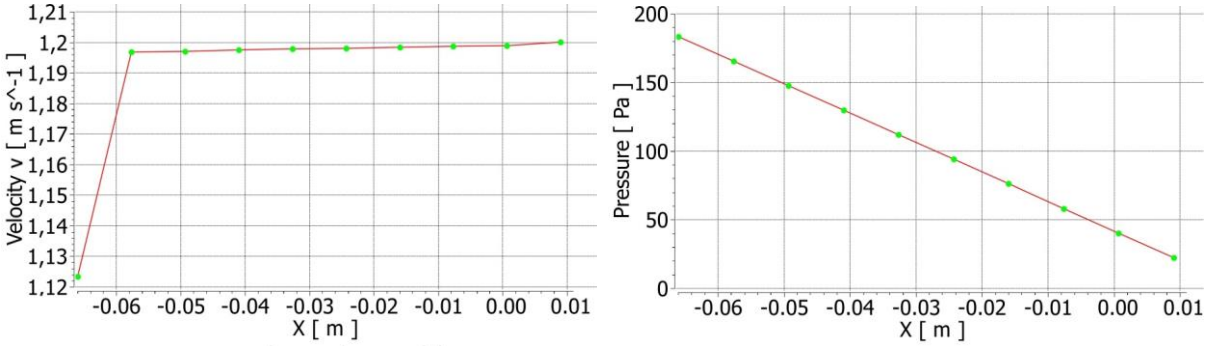

Figure 13. Parameters of flow through monolith of prototype A: a) velocity, b) static pressure.

Finally the earlier CFD simulation for ambient temperature (300 K) and simulation for inlet side temperature 773 K were compared. As can be seen in figure 14, the difference in pressure drop is significant and a place, where the temperature fields are the highest, is around the monolith, which is desirable due to the positive effect of the temperature on conversion of harmful substances.

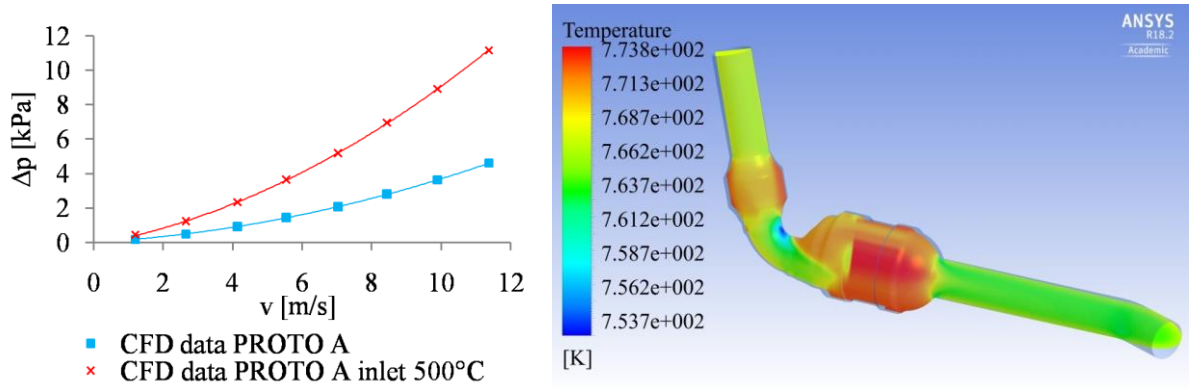

Figure 14. Increasing temperature at inlet for prototype A: comparison (left), temp. fields (right).

6. Summary

Increasingly stricter requirements for emissions standards, force the manufacturers of exhaust systems of both, the first assembly (OEM part) and the spare parts (replacement part for aftermarket), to apply new technologies and intensify research around them. One of these solutions that help to know better the behaviour of flow (static pressure, velocity and temperature fields) inside the catalysts is CFD.

This study shows the differences in flow through the catalysts after using a different geometry and monoliths, compared to the original part. Using another similar part (cone) at inlet side, affects the distribution of gas to the substrate. However, in this case maintained a similar uniformity index, as in the original part, was maintained. Furthermore, simulations allowed to predict which prototype with a monolith has a similar pressure drop as in the original part and these are prototype B, E, C and on the limit A and D. Prototype F had a high pressure drop due to higher CPSI value of monolith, which is caused by lower porosity (OFA – Open Front Area or also called void fraction).

Experimental and numerical analysis allowed to choose the appropriate prototypes for further testing in a certified unit that carries out backpressure and emission tests in order to obtain approval for WALKER catalytic converters.

References

[1] Postrzednik S and Żmudka Z 2007 *Termodynamiczne oraz ekologiczne uwarunkowania eksploatacji tłokowych silników spalinowych* Wydawnictwo Politechniki Śląskiej (Gliwice)
[2] Rokosch U 2007 *Układy oczyszczania spalin i pokładowe systemy diagnostyczne samochodów* Wydawnictwa Komunikacji i Łączności (Warszawa)
[3] Pardiwala J M, Patel F and Patel S 2011 *Review paper on catalytic converter for automotive exhaust emission* Int. Conf. on Current Trends in Technology, NUiCONE (India: Ahmedabad) pp 1-6
[4] Borzęcka A 2012 *Monolithic catalysts – current and future applications, Interdyscyplinarne zagadnienia w inżynierii i ochronie środowiska* vol 2, ed T M Traczewska, Oficyna Wydawnicza Politechniki Wrocławskiej (Wrocław) pp 81-87
[5] Bertrand F, Devals C, Vidal D, Séguineau de Préval C and Hayes R E 2012 Towards the simulation of the catalytic monolith converter using discrete channel-scale models *Catalysis Todat* **188** pp 80-86
[6] Holder R, Bollig M, Anderson D R and Hochmuth J K 2006 A discussion on transport phenomena and three-way kinetics of monolithic converters *Chemical Engineering Science* **61** pp 8010-8027
[7] Żmudka Z and Postrzednik S 2011 Inverse aspects of the three-way catalytic converter operation in the spark ignition engine *Journal of KONES* **18** pp 509-516
[8] Roy M M, M U H Joardder and M S Uddin 2010 *Effect of engine backpressure on the performance and emissions of a CI engine* JIMEC'7 (Amman - Jordan) pp 1-7
[9] Ramganesh R and Devaradjane G 2015 *Simulation of flow and prediction of back pressure of the silencer using CFD* Jurnal of Chemical and Pharmaceutical Sciences (India) pp 297-300
[10] Żmudka Z and Postrzednik S 2006 Catalytic converter as an element of flow resistance in engine exhaust system *Journal of KONES* **132** pp 207-216
[11] Priyadarsini Ch I, Modali M, Krishna S V and Reddy N D 2016 Design and analysis of muffler to reduce the back pressure *Int. Journal of Scientific Res. Engin. & Technol.* **5** pp 470-474
[12] Puneetha C G, Manjunath H and Shashidhar M R 2015 *Backpressure study in exhaust muffler of single cylinder diesel engine using CFD analysis* Altair Technology Conf. (India) pp 1-14
[13] Amirnordin S H, Seri S M, Salim W S-I W, Rahman H A and Hasnan K 2011 Pressure drop analysis of square and hexagonal cells and its effect on the performance of catalytic converters *Int. Journal of Environmental Science and Development* **2** pp 239-247
[14] Raja V and Fernandes K J 2008 *Reverse engineering: an industrial perspective* Springer (UK)
[15] Ibrahim H A, Abdou S and Ahmed W H 2017 *Understanding flow through catalitic converters* Int. Conf. of Fluid Flow, Heat and Mass Transfer (Toronto) pp 1-7
[16] Liu B, Hayes R E, Yi Y, Mmbaga J, Checkel M D and Zheng M 2007 Three dimensional modelling of methane ignition in a reverse flow catalitic converter *Computers and Chemical Engineering* **31** pp 292-306
[17] Nowak R 2016 Estimation of viscous and inertial resistance coefficients for various heat sink configurations *Procedia Engineering* **157** pp 122-130
[18] Karuppusamy P and Senthil R 2013 Design, analysis of flow characteristics of catalytic converter and effects of backpressure on engine performance *Int. Journal of Research in Engineering & Advanced Technology* **1** pp 1-6

Acknowledgments

First of all, I would like to special thanks to my Tenneco company for the possibility to carry out research in the laboratory of flow and 3D. In addition, my direct management of Aftermarket for financing the entire project. I am grateful also to my promoters (co-authors) from Silesian University of Technology for technical support.

This scientific work was partly supported by Faculty of Power and Environmental Engineering of the Silesian University of Technology within the statutory research.